Cell Tissue Res (2015) 362:597–609
DOI 10.1007/s00441-015-2228-2

REGULAR ARTICLE

Endothelial juxtaposition of distinct adult stem cells activates angiogenesis signaling molecules in endothelial cells

Elham Mohammadi[1] · **Seyed Mahdi Nassiri**[1] · **Reza Rahbarghazi**[2] · **Vahid Siavashi**[3] · **Atefeh Araghi**[4]

Received: 17 March 2014 / Accepted: 22 May 2015 / Published online: 12 June 2015

Abstract Efficacy of therapeutic angiogenesis needs a comprehensive understanding of endothelial cell (EC) function and biological factors and cells that interplay with ECs. Stem cells are considered the key components of pro- and anti-angiogenic milieu in a wide variety of physiopathological states, and interactions of EC-stem cells have been the subject of controversy in recent years. In this study, the potential effects of three tissue-specific adult stem cells, namely rat marrow-derived mesenchymal stem cells (rBMSCs), rat adipose-derived stem cells (rADSCs) and rat muscle-derived satellite cells (rSCs), on the endothelial activation of key angiogenic signaling molecules, including VEGF, Ang-2, VEGFR-2, Tie-2, and Tie2-pho, were investigated. Human umbilical vein endothelial cells (HUVECs) and rat lung microvascular endothelial cells (RLMECs) were cocultured with the stem cells or incubated with the stem cell-derived conditioned media on Matrigel. Following HUVEC-stem cell coculture, CD31-positive ECs were flow sorted and subjected to western blotting to analyze potential changes in the expression of the pro-angiogenic signaling molecules. Elongation and co-alignment of the stem cells were seen along the EC tubes in the EC-stem cell cocultures on Matrigel, with cell-to-cell dye communication in the EC-rBMSC cocultures. Moreover, rBMSCs and rADSCs significantly improved endothelial tubulogenesis in both juxtacrine and paracrine manners. These two latter stem cells dynamically up-regulated VEGF, Ang-2, VREGR-2, and Tie-2 but down-regulated Tie2-pho and the Tie2-pho/Tie-2 ratio in HUVECs. Induction of pro-angiogenic signaling in ECs by marrow- and adipose-derived MSCs further indicates the significance of stem cell milieu in angiogenesis dynamics.

Keywords Angiogenesis · Endothelial cell · Stem cell · Coculture · Signaling

Introduction

Angiogenesis or the formation of new capillaries from pre-existing vessels is a dynamic phenomenon with juxtacrine or paracrine cross-talks between endothelial cells (ECs) and their spatially distinct microenvironment, including neighboring cells, signals, and extracellular matrix (ECM) (Boomsma and Geenen 2012; Davis and Senger 2005; Rahbarghazi et al. 2013). To date, numerous in vivo and in vitro experimental studies have been carried out to illuminate the underlying mechanisms behind physiological and pathological neo-angiogenesis. Stem cells are touted as the key regulators of neo-angiogenesis through dynamic interactions with ECs in a context-dependent manner in different physiopathological conditions (Nassiri and Rahbarghazi 2014). In this regard, tissue-derived stem cells, especially bone marrow-derived mesenchymal stem cells (BMSCs), adipose-derived stem cells

Electronic supplementary material The online version of this article (doi:10.1007/s00441-015-2228-2) contains supplementary material, which is available to authorized users.

✉ Seyed Mahdi Nassiri
nasirim@ut.ac.ir; nasirim@vetmed.ut.ac.ir

[1] Department of Clinical Pathology, Faculty of Veterinary Medicine, University of Tehran, P.O Box: 14155-6453, Qareeb St., Azadi Ave., Tehran, Iran

[2] Stem Cell Research Center, Tabriz University of Medical Sciences, Tabriz, Iran

[3] Department of Biology, Faculty of Sciences, University of Guilan, Rasht, Iran

[4] Faculty of Veterinary Medicine, Amol University of Special Modern Technologies, Amol, Iran

(ADSCs), and muscle-derived satellite cells (SCs), have been extensively investigated for angiogenesis-based regeneration with some attempts undertaken to unveil the corresponding mechanisms. Accumulating evidence from different experiments suggests that these cells are emerging as therapeutics for the augmentation of angiogenesis in some pathologies such as prolonged myocardial and muscular ischemia (Mima et al. 2012; Sambasivan et al. 2011; Tang et al. 2009). In the coculture of rat SCs and microvascular fragments, the index of angiogenesis was greater than that of single cell culture (Rhoads et al. 2009). Moreover, ADSCs and SCs were able to promote angiogenesis through cytokine and protease expression (Kachgal and Putnam 2011). Meanwhile, the topical administrations of orbital fat-derived stem cells contributed to corneal regeneration through the modulation of inflammation and trans-differentiation into epithelial-like cells (Agorogiannis et al. 2012). In a recent study, we also showed some pro-angiogenic properties of BMSCs and SCs in vivo and in vitro (Rahbarghazi et al. 2013). The molecular analysis and secretome profile of BMSCs revealed that a variety of soluble factors, including vascular endothelial growth factor (VEGF), vascular endothelial growth factor receptor 2 (VEGFR2), and Tie2, are secreted into their conditioned medium. However, the biological effects of these signaling molecules have yet to be determined in angiogenesis dynamics (Baraniak and McDevitt 2010; Nassiri and Rahbarghazi 2014; Rahbarghazi et al. 2013). Despite the pro-angiogenic effect of BMSCs on ECs, some MSC-derived anti-angiogenic properties were reported by some authors, and a number of conditions, including connexin-43 expression and reactive oxygen species production, were considered prone to the anti-angiogenic effect of MSCs (Otsu et al. 2009; Villars et al. 2002), which could be of therapeutic relevance in certain pathologies such as tumor growth (Nassiri and Rahbarghazi 2014). For example, Ho et al. (2013) found that the co-administration of BMSCs and glioma cells into immuno-deficient mice resulted in a reduction in tumor size and microvessel formation.

Understanding the different interactions between stem cells and ECs and the role of stem cells in the tissue microenvironment under physiological and pathological conditions as well as the kinetics of pro-angiogenic signaling molecules is indispensable during development of new stem cell-based pro- or anti-angiogenic therapeutic strategies (Nassiri and Rahbarghazi 2014). Under relative control, designing coculture systems can be helpful to elaborate the reciprocal cell–cell interactions in angiogenesis dynamics (Aguirre et al. 2010). The present study sought to comparatively investigate the effects of three types of adult stem cells, namely rat BMSCs (rBMSCs), rat SCs (rSCs), and rat ADSCs (rADSCs), on the kinetics of key angiogenic signaling molecules in ECs in order to determine the potential signaling pathways that each of these stem cells may dynamically induce in ECs and to compare the potency of these three types of stem cells for switching on a special angiogenic signaling pathway in ECs.

Materials and methods

Animals

In the present study, both green fluorescent protein (GFP)-positive (rat$^{GFP+/+}$) ([Wistar-TgN (CAG-GFP) 184ys] strain) and GFP-negative adult male Wistar rats (rat$^{GFP-/-}$) were used (Hakamata et al. 2001; Rahbarghazi et al. 2013). The rats, weighing 80–100 g, were treated in accordance with the published guidelines of The Care and Use of Laboratory Animals (NIH Publication No. 85–23, revised 1996). All phases of this study were approved by the Animal Care Committee of the University of Tehran.

Cell isolation and expansion

Human umbilical vein endothelial cells

Human umbilical vein endothelial cells (HUVECs) were isolated from the umbilical vein as previously described (Baudin et al. 2007; Marin et al. 2001). Umbilical cords were obtained from normal placentas with no gross abnormalities and without hepatitis or HIV contamination. For each cord, the vein was cannulated with sterile blunt needles and the needles were fixed with a sterile string. The vein was perfused with phosphate-buffered saline (PBS), then filled with 0.2 % collagenase type I solution (Catalog No. C0130; Sigma-Aldrich), placed into a bottle containing sterile 0.15 M NaCl and incubated at 37 °C for 15 min in the water bath. The suspension of ECs was flushed from the cord by perfusion with 40 ml 1× PBS into a tube containing 10 ml culture medium and centrifuged at 750*g* for 10 min. Then, the cell pellet was re-suspended in 5 ml M199 medium (Catalog No. M5017; Sigma-Aldrich) supplemented with 20 % fetal bovine serum (FBS; Catalog No. 10270; Gibco-Invitrogen), 1 % L-glutamine (Catalog No. 25030–081; Gibco-Invitrogen), 1.5 % 1 M HEPES (Catalog No. H3375; Sigma-Aldrich), and 100 IU/ml penicillin-100 mg/ml streptomycin (Catalog No. 15140–122; Gibco-Invitrogen), then plated in 25-cm^2 gelatin-coated plastic cell culture flasks (Catalog No. 70025; SPL Life Science) and incubated at 37 °C in a 95 % air/5 % CO_2 atmosphere. The culture medium was replaced after 24 h, and then every 2 days until confluency. At contact inhibition, the EC cultures displayed a cobblestone appearance by the phase-contrast microscopy.

Rat lung microvascular endothelial cells

Rat lung microvascular endothelial cells (RLMECs) were isolated from the peripheral lung tissue as previously described with some modifications (Magee et al. 1994). Briefly, the lungs were excised under aseptic conditions from the sacrificed rats and the outer 3–5 mm of the peripheral lung

lobes were dissected from the remaining tissue, gently minced, washed with PBS, and incubated in 2 mg/ml collagenase type I solution at 37 °C for 45 min on a rotator. Subsequently, the suspension was centrifuged at 200*g* for 5 min and the pellet was resuspended in endothelial cell growth medium (M199 supplemented with Endothelial Cell Growth Medium MV2 SupplementPack; Catalog No. 39221; PromoCell) containing 5 ng/ml epidermal growth factor (EGF), 10 ng/ml basic fibroblast growth factor (bFGF), 20 ng/ml insulin-like growth factor (IGF), 0.5 ng/ml VEGF, 1 μg/ml ascorbic acid and 0.2 μg/ml hydrocortisone together with 10 % FBS and 100 IU/ml penicillin-100 mg/ml streptomycin), then passed through a 100-μm nylon mesh, plated in a 25-cm^2 cell culture flask and incubated in a humidified incubator at 37 °C with 5 % CO_2. The medium was changed after 24 h to remove non-adherent and dead cells. After 48 h, the cells were refed with L-valine free media (Catalog No. M 7395; Sigma Aldrich) supplemented with Endothelial Cell Growth Medium MV2 SupplementPack, 10 % FBS, 1.2 mg/l D-valine (Catalog No. V1255; Sigma Aldrich) and 100 IU/ml penicillin-100 mg/ml streptomycin. Passage 3 cells were used for our experiments.

Rat bone marrow mesenchymal stem cells

Rat marrow-derived mesenchymal stem cells (rBMSCs) were isolated from healthy adult rats and expanded as previously described (Barbash et al. 2003; Deng et al. 2010). Briefly, the femur and tibia were aseptically excised. After removing all connective tissues attached to bones, the epiphyses were removed, and then an 18-gauge needle was inserted into the medullary cavity and medullary components were flushed with 2 ml culture medium. Next, the medullary components were layered onto an equal volume of Ficoll-Hypaque (Catalog No. 10771; Sigma-Aldrich) and centrifuged at 400*g* for 30 min. Bone marrow mononuclear cells were subsequently isolated from the gradient interface, washed with PBS, resuspended in Dulbecco's Modified Eagle's Medium-low glucose (DMEM/LG; Catalog No. 31600; Gibco-Invitrogen) containing 20 % FBS, 100 IU/ml penicillin-100 mg/ml streptomycin, plated in 25-cm^2 culture flasks, and incubated at 37 °C humidified atmosphere with 5 % CO_2. Hematopoietic cells were discarded during routine medium replacement. Passage 3 cells were used in our experiments.

Rat adipose tissue-derived stem cells

Rat adipose tissue-derived stem cells (rADSCs) were isolated from subcutaneous inguinal adipose tissues as previously described (Meligy et al. 2012; Taha and Hedayati 2010). Briefly, adipose tissues were aseptically harvested from the inguinal region and cut into small pieces. The pieces were then digested with 0.1 % collagenase type I at 37 °C for 30 min to obtain cell suspension. The suspension was filtered through a 70-μm-diameter mesh to remove tissue debris. After centrifugation (1200 rpm, 10 min), the cell pellet was suspended in DMEM/LG containing 20 % FBS, 100 IU/ml penicillin-100 mg/ml streptomycin. The culture media was changed every 2 days, and passage 3 cells were used for our experiments.

Rat satellite cells

Rat muscle satellite cells (rSCs) were obtained from the hindlimb muscles of the adult rats as was previously described with some modifications (Danoviz and Yablonka-Reuveni 2012; Rhoads et al. 2009). Briefly, after euthanasia, tibialis anterior and gastrocnemius muscles were harvested from both hind limbs and the tendons, fat, vessels, and connective tissues were carefully removed as far as possible. Subsequently, the muscles were pulverized into small fragments and incubated in 0.1 % collagenase type I in DMEM at 37 °C for 60 min. At the end of the digestion period, the enzyme solution containing tissue fragments was centrifuged at 400*g* for 5 min. After aspirating the supernatant, 5 ml DMEM containing 10 % FBS was added, and mechanical trituration was performed to release still attached satellite cells. Afterwards, the supernatant from the trituration was passed through a 40-μm mesh to eliminate residual large debris. After centrifugation, the cell suspension was transferred to DMEM/HG (Catalog No. 12800-116; Gibco-Invitrogen) supplemented with 15 % FBS, 5 % horse donor serum, and 10 ng/ml bFGF (Catalog No. f0291; Sigma-Aldrich) and incubated at 37 °C, 95 % relative humidity, and 5 % CO2 in an incubator, where it was not disturbed for 3 days before the first medium exchange. Passage 3 cells were used for the experiments.

Flow cytometry

The third passage of rBMSCs, rADSCs, HUVECs and RLMECs was trypsinized and subjected to flow cytometry to determine the expression level of cellular CD markers. Flow cytometry analysis was performed with a panel of antibodies, including mouse anti-CD90-fluorescein isothiocyanate (FITC; Catalog No. ab11155; Abcam), mouse anti-CD105-FITC (Catalog No. ab53318; Abcam), mouse anti-CD44-FITC (Catalog No. MCA643F; AbD Serotec), mouse anti-CD34-FITC (Catalog No. SC-7324; Santa Cruz Biotechnology), rabbit anti-CD45 (Catalog No. ab10558; Abcam), and mouse anti-CD31 (Catalog No. sc-80913; Santa Cruz Biotechnology). Isotype control antibodies included mouse IgG_{2a} isotype control-FITC (Catalog No. 14–4724; eBioscience), mouse IgG_1 isotype control-FITC (Catalog No.11-4714; eBioscience), rabbit IgG isotype control (Catalog No. ab27472; Abcam), and mouse IgG1 (Catalog No. sc-3877; Santa Cruz Biotechnology). Goat anti-rabbit IgG-

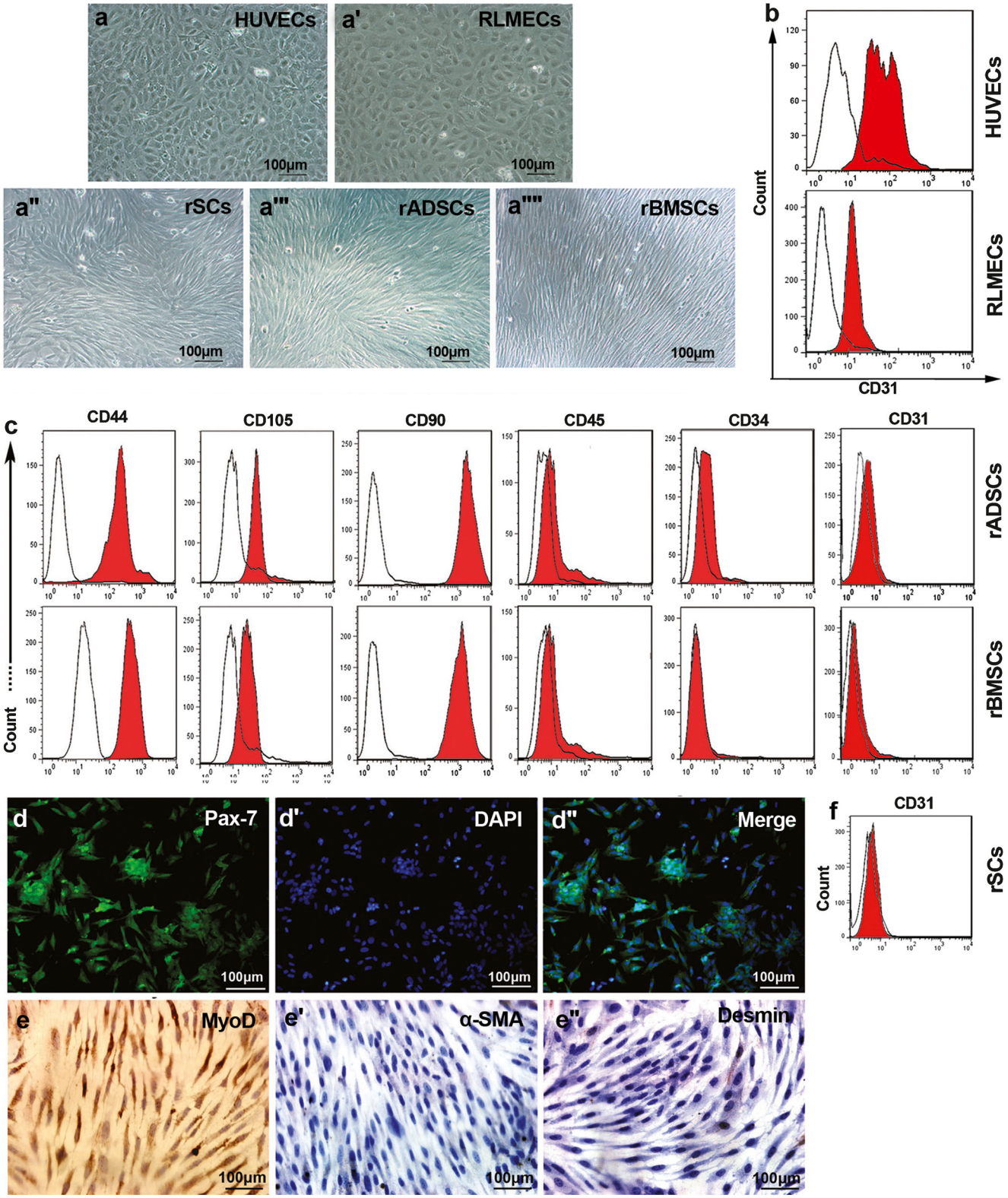

phycoerythrin (PE; Catalog No. ab97070; Abcam) and goat anti-mouse IgG1-PerCP-Cy5.5 (Catalog No. sc-45103; Santa Cruz Biotechnology) were used as secondary antibodies against unconjugated primary antibodies. Flow cytometry was performed by FACSCalibur (BD Bioscience), and the output data were analyzed with the FlowJo software (v.7.6.1).

◀ **Fig. 1** Cell characterization. Phase-contrast micrographs of the confluent monolayer of the cells (passage 3) (**a**–**a''''**). HUVECs (**a**) and RLMECs (**a'**) exhibit a cobblestone, polygonal appearance with prominent nucleoli in a flat layer, whereas rSCs (**a''**), rADSCs (**a'''**), and rBMSCs (**a''''**) are characterized by flattened, fibroblast-like morphology with a whirlpool growth pattern. Flow cytometric histograms of CD31 expression by HUVECs and RLMECs (**b**). Immunophenotypic characterization of rADSCs and rBMSCs by flow cytometry (**c**). Both rADSCs and rBMSCs are positive for CD44, CD105, and CD90, but they are negative for CD34, CD45, and CD31 (**c**). The colorless histograms show the profile of the isotype control. Immunofluorescence and immunocytochemistry stainings of rSCs show the expression of Pax-7 (**d**–**d''**) and MyoD (**e**) and negative staining for alpha-smooth muscle actin (**e'**) and desmin (**e''**). rSCs were also characterized as CD31 negative (**f**). *Scale bar* (**a**–**a''''**, **d**–**d''** and **e**–**e''**) 100 μm

Immunofluorescence

The rSCs were seeded in 4-well glass-slide chambers. The cultures were rinsed with PBS-Tween 20 (0.05 %) for 5 min, fixed with 4 % paraformaldehyde (PFA) at room temperature for 20 min, and permeabilized with 0.5 % Triton X-100 in PBS for 10 min at room temperature. After rinsing with PBS-Tween 20, the blocking solution (5 % bovine serum albumin (BSA) in PBS) was added and incubated for 1 h to block non-specific antibody binding. The cells were then incubated overnight at 4 °C with the following primary antibodies: mouse anti-Pax-7 (1:200; Developmental Studies Hybridoma Bank, University of Iowa, USA) and mouse anti-MyoD (5 mg/mL dilution, Catalog No. 554130; BD Pharmingen). After washing the cells with PBS-Tween 20, FITC conjugated goat anti-mouse IgG_1 (1:3,000, Catalog No. ab6785; Abcam) secondary antibody was applied for 1 h in a dark humidified chamber at room temperature. Finally, the cells were washed three times with 0.05 % Tween-PBS solution (15 min each time). Additionally, 4-6-Diamidino-2-phenylindole (DAPI, 300nM in PBS) (Catalog No.D8417; Sigma-Aldrich) was used for nuclear counterstaining. The prepared mounts were imaged using a fluorescent microscope (DP72; Olympus), and the images were merged and processed by DP2-BSW software (v.2.2). Anti-desmin (Catalog No. M0760; Dako), anti-MyoD (Catalog No. M3512; Dako), and anti-alpha-smooth muscle actin (α-SMA) (Catalog No. M0851; Dako) antibodies were used for immunocytochemistry. Counterstain with hematoxylin was used to identify the nuclei.

Collection of conditioned media

In order to investigate the paracrine effects of rBMSCs, rADSCs, and rSCs on tubulogenesis of ECs, stem cell-conditioned media (CM) was collected in a period of 24 h. After 70–80 % cell confluency in T25 culture flasks, the culture medium was aspirated and the cells were washed three times with PBS to remove serum remnants. Next, 5 ml serum-free M199 medium was added to the cells and incubated for 24 h (Hsiao et al. 2012; Kinnaird et al. 2004). Then, the CM was collected, centrifuged at 1000*g* for 10 min, and filtered through a 0.2-μm filter (GVS Filter Technology). The harvest was stored at −80 °C until use.

EC fluorescent staining with CM-Dil

The ECs were labeled with Cell Tracker™ CM-Dil (Catalog No. C-7000; Molecular Probes) to facilitate EC tracking in EC-stem cell coculture experiments. For this purpose, the cells were incubated with 2 μM of the dye for 20 min at 37 °C, washed with PBS, trypsinized, washed with PBS, and resuspended in M199 medium (Sorrell et al. 2009).

In vitro tube formation assay

Tube formation assay was carried out by using growth factor depleted Matrigel (Catalog No. 356231; BD Biosciences). Two types of ECs, including HUVECs and RLMECs, were used for Matrigel tube formation assays. Briefly, 96-well plates (Catalog No. 167008; Nunclon) were coated with 50 μl per well of Matrigel diluted in M199 medium (1:1 ratio) and incubated at 37 °C for 30 min to solidify. For each type of ECs, two separate experiments were designed to perform the in vitro tube formation assay: (1): ECs (2×10^4 cells per well) with 200 μl of either M199 medium, rBMSCs-CM, rADSCs-CM, or rSCs-CM, supplemented with 1 % FBS; and (2) co-culture experiments with 16,000 ECs+4000 either rBMSCs, rADSCs, or rSCs (EC-stem cell ratio of 4:1) in 200 μl M199 medium supplemented with 1 % FBS. After 16 h of incubation, the cells were photographed and analyzed (Salvucci et al. 2002). Immediately after seeding on Matrigel, the ECs colonized and then started sprouting and elongating (Rahbarghazi et al. 2013). In vitro tubulogenesis was assessed using a colony scoring system according to our previous study (Rahbarghazi et al. 2013). Briefly, 25 colonies in each well were examined and a 0–4 score was allocated to each colony as follows: 0, aggregate with no sprouting; 1, colony sprouting without arborization; 2, with arborization; 3, with anastomosis; and 4, development of a complex network. For each well, the total score was calculated by adding all the 25 scores, with a maximum possible score of 100. The average tubular length from 10 serial microscopic fields per well was also measured using ImageJ software. Fluorescent images were captured with an inverted microscope (Olympus IX71) and merged using analysis LS Starter software.

Proliferation assay

In order to comparatively assess whether tissue-specific stem cells had any proliferative effect on ECs in the EC-stem cell coculture systems, GFP-positive rat stem cells were cocultured with HUVECs, which were prelabeled with red

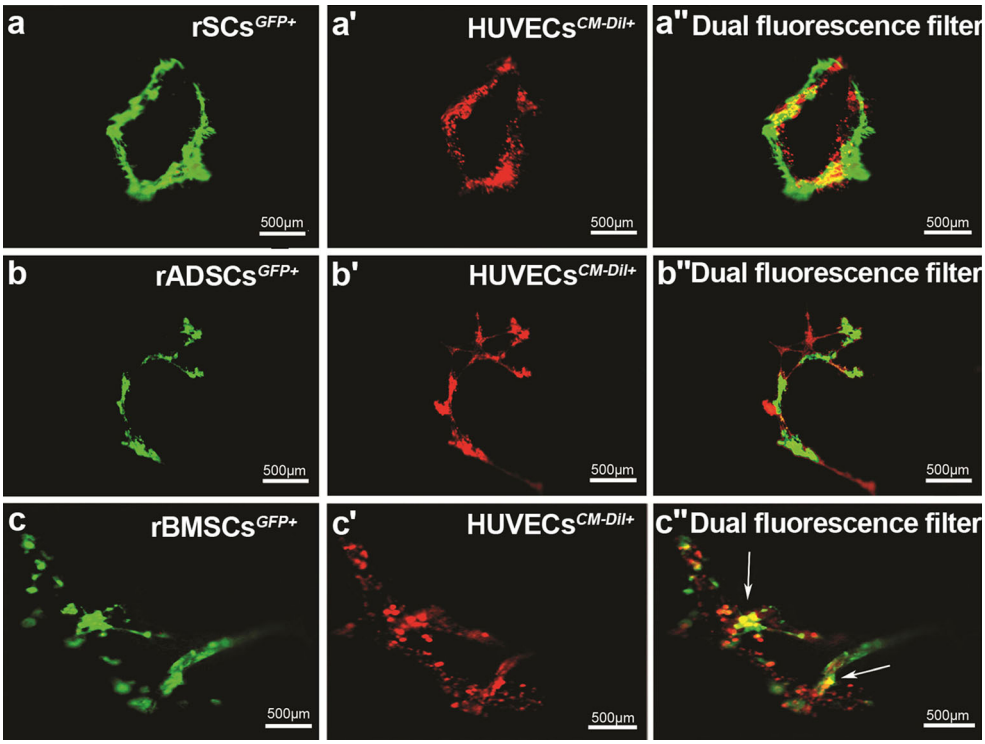

Fig. 2 Representative images of juxtaposed rSCs$^{GFP+/+}$ (**a**), rADSCs$^{GFP+/+}$ (**b**), and rBMSCs$^{GFP+/+}$(**c**) with HUVECs$^{CM\text{-}DiI+}$ (a', b', and c') in Matrigel tube-like arrays. In all cocultures, the GFP-positive cells align along the red-fluorescent-labeled HUVECs to establish well-formed vascular networks (**a"**, **b"**, and **c"**). In the EC-rBMSC coculture, dual fluorescent cells (*yellow*) are seen by dual-fluorescence filter (**c"**, *white arrows*). These tissue-specific stem cells are able to intercalate with ECs and stabilize capillary-like structures

fluorescent dye CellTracker™ CM-DiI. For this assay, the fluorescently-labeled HUVECs were first serum-starved in M199 containing 1 % FBS overnight. Then, the ECs were harvested and cocultured with rat stem cells in Matrigel-coated 24-well plates at an EC-stem cell ratio of 4:1 in M199 containing 1 % FBS. After 48 h, the cells were harvested, resuspended in 0.5 ml PBS, and counted under a fluorescent microscope to determine the number of ECs and stem cells in each coculture.

Three-dimentional coculture

In order to analyze the potential effects of rBMSCs, rADSCs, and rSCs on angiogenic signaling molecules in ECs, a three-dimensional coculture system was used on Matrigel in 6-well dishes. For this purpose, HUVECs-stem cells were mixed (4:1 ratio) in M199 medium with 1 % FBS and seeded on Matrigel-coated wells. For control conditions, ECs were cultured alone on Matrigel in M199 medium with 1 % FBS.

Cell sorting and western blotting

To evaluate the kinetics of angiogenic-signaling molecules, HUVECs at 16, 24, and 48 h after coculture were subjected to western blot analysis. Prior to cell lysis, the ECs were purified for CD31 expression (Catalog No. 14-0319-82; eBioscience) by flow sorting using FACSAria (Becton Dickinson, USA) cell sorter system. Total protein was extracted from 1.2×10^6 ECs using PRO-PRE™ Protein Extraction Solution (Catalog No.17801; iNtRON Biotechnology, Seongnam, Korea), and then protein concentration was determined with the SMART™ Micro BCA Protein Assay kit (Catalog No. 21071; iNtRON Biotechnology) by Smartspec Plus spectrophotometer (Bio-Rad). Subsequently, 40 μg of cell lysate (under reducing condition) was loaded on SDS-PAGE gels (5 % stacking and 10 % separating gels) and then transferred to 0.2 μm immune-Blot™ polyvinylidenedifluoride (PVDF) membranes (Catalog No. 162–017777; Bio-Rad Laboratories, CA, USA). The membranes were blocked with 3 % non-fat dry milk (Catalog No. 1.15363.0500; Merck, Darmstadt, Germany) or 5 % BSA (Catalog No. A-7888; Sigma-Aldrich, MO, USA) in Tris-buffered saline containing 0.1 % Tween 20 (TBST), for 1 h in accordance with the manufacturer's recommendations and then immunoblotted with primary antibodies for 1 h at room temperature. Antibodies used in western blot assays were as follows: mouse anti-VEGF (5 μg/mL, Catalog No. ab1316; Abcam), rabbit anti-VEGF receptor 1

Fig. 3 Effects of tissue-derived stem cells and their conditioned media (CM) on the tube formation of HUVECs. A significantly higher Matrigel tubulogenesis scoring (**e**) and a greater tube length (**f**) was recorded when HUVECs were juxtaposed with marrow- (**d**) or adipose-derived stem cells (**c**), whereas HUVECs-rSCs interaction (**b**) did not change the endothelial Matrigel tube formation compared with HUVECs only (**a**). Conditioned media from marrow- (**j**) and adipose-derived stem cells (**i**) had a superior effect on the Matrigel tube formation of HUVECs (**k**, **l**). Lumens are shown by the *asterisks*. Data are expressed as mean±SD (three independent experiments were performed in triplicate). *$P<0.05$, **$P<0.01$ (One-way ANOVA with Bonferroni post hoc test)

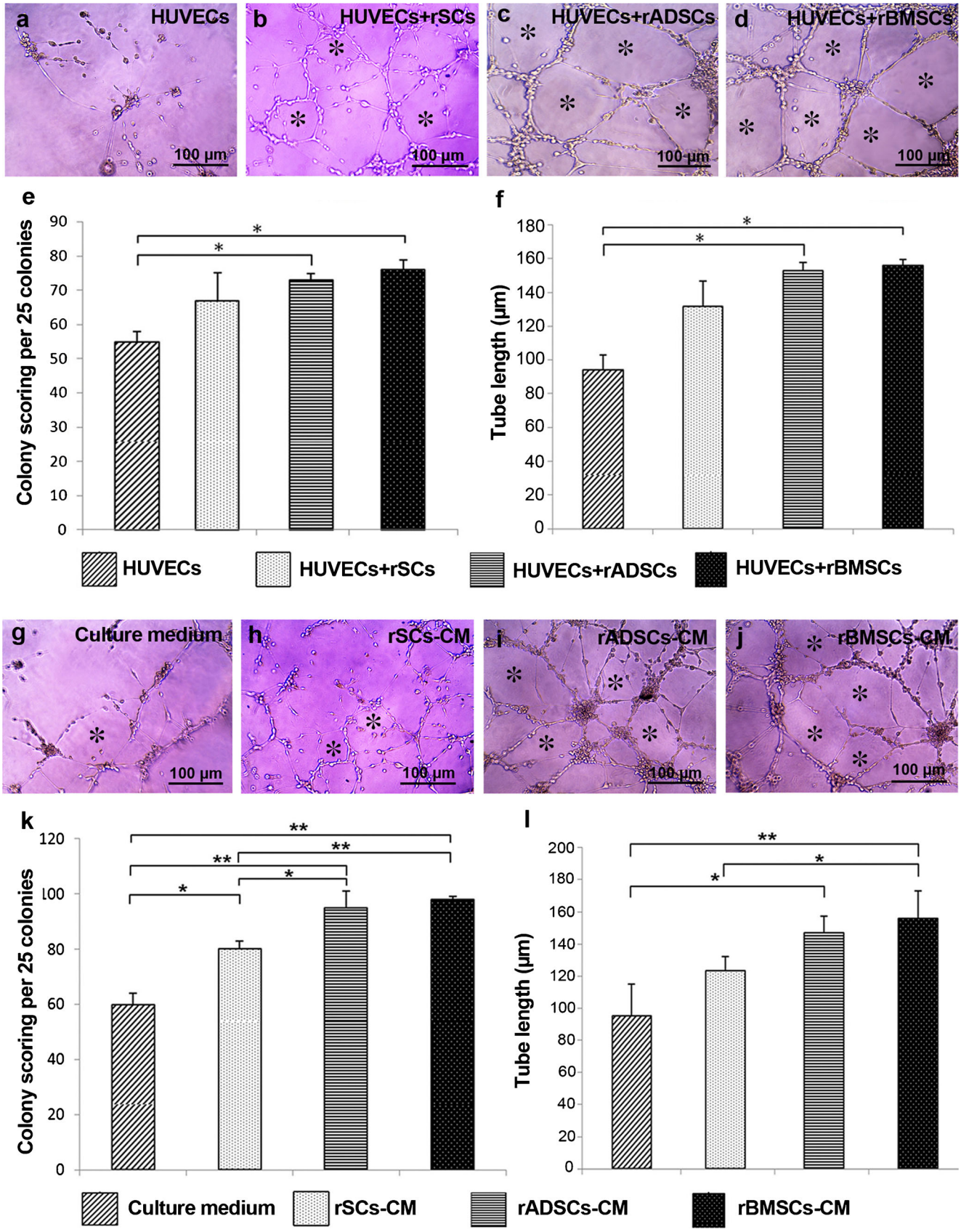
a HUVECs
100 μm
b HUVECs+rSCs
100 μm
c HUVECs+rADSCs
100 μm
d HUVECs+rBMSCs
100 μm
e
Colony scoring per 25 colonies
0
10
20
30
40
50
60
70
80
90
*
*
f
Tube length (μm)
0
20
40
60
80
100
120
140
160
180
*
*
HUVECs
HUVECs+rSCs
HUVECs+rADSCs
HUVECs+rBMSCs
g Culture medium
100 μm
h rSCs-CM
100 μm
i rADSCs-CM
100 μm
j rBMSCs-CM
100 μm
k
Colony scoring per 25 colonies
0
20
40
60
80
100
120
*
*
*
**
**
**
l
Tube length (μm)
0
20
40
60
80
100
120
140
160
180
200
*
*
**
Culture medium
rSCs-CM
rADSCs-CM
rBMSCs-CM

(1:10000, Catalog No. ab32152; Abcam), rabbit anti-VEGF receptor 2 (1 μg/mL, catalog No. ab39256; Abcam), rabbit anti-angiopoietin 1 (1 μg/mL, Catalog No. ab95230; Abcam), rabbit anti-angiopoietin 2 (1 μg/ml, Catalog No. ab65835; Abcam), mouse anti-Tie1 (2 μg/mL, Catalog No. ab27851; Abcam), mouse anti-Tie2 (1 μg/mL; Catalog No. ab24859; Abcam), rabbit anti-phospho-Tie2 (1:1000, Catalog No. ab78142; Abcam), and mouse anti-beta actin-loading control (1 μg/mL, Catalog No. ab8224; Abcam). Bound antibodies were detected using horseradish peroxidase (HRP)-conjugated secondary antibodies, including rabbit anti-mouse IgG-HRP (1:4000; Catalog No. ab6728; Abcam) and sheep anti-rabbit IgG-HRP (1:5000, catalog No. ab6795; Abcam). A solution containing 0.006 % 3, 3'-diaminobenzidine (DAB) (Catalog # D5637; Sigma-Aldrich) was used for immunoblot protein detection according to the manufacturer's instruction. The films were scanned using an HP Scanjet G3110 apparatus (Hewlett-Packard, CA, USA). Finally, the quantification of each band was accomplished by the corresponding densitometry of the actin band using ImageJ v.1.44p software (NIH, USA) as described previously (Rahbarghazi et al. 2013). The area (%) under the curve of each band was divided by the corresponding percentage of the area under the curve of the actin band, and the calculated values were compared statistically between groups.

Statistical analysis

Statistical analysis was carried out by SPSS software v.16 (SPSS, Chicago, IL, USA), and the data were presented as mean±standard deviation (SD). One-way ANOVA, followed by Bonferroni's post hoc comparison test, was used to analyze the results of the experiments. The mean difference was significant at $P<0.05$. In histograms, statistical difference between the groups is shown by brackets with $*P<0.05$, $**P<0.01$, and $***P<0.001$.

Results

Cell characterization

HUVECs and RLMECs at passage 3 (Fig. 1) were subjected to flow cytometry to test the expression level of CD31. Flow cytometric immunophenotyping showed that both types of the cultured ECs expressed CD31 (Fig. 1b), whereas the adult stem cells used in this study were CD31 negative (Fig. 1c, f). For the rBMSCs and rADSCs, the immunophenotyping of the cultured cells revealed the expression of several stemness molecules, including CD44, CD90, and CD105. These cells were negative for CD34 and CD45 (Fig. 1c). In addition, α-SMA immunostaining of the HUVECs, RLMECs, rADSCs, and rBMSCs revealed that these cells were negative for α-SMA (Supplementary Fig. 1). Meanwhile, immunostaining of the rSCs revealed the co-expression of Pax-7 (1d) and MyoD (1e), whereas these cells were α-SMA- and desmin-negative (Fig. 1e', e").

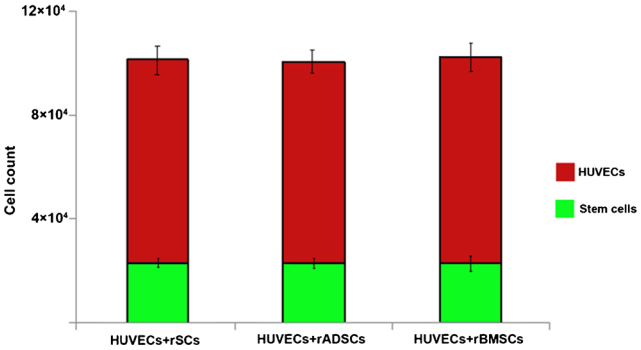

Fig. 4 Effects of adult stem cells on the proliferation of endothelial cells. 8×10^4 red-fluorescent-labeled HUVECs were cocultured with 2×10^4 GFP-positive rat stem cells. After 48 h, the cells were harvested and counted under a fluorescent microscope. No difference was observed in the number of ECs and stem cells or in the ratio of ECs to stem cells between different cocultures. Data are expressed as mean±SD (two independent experiments were performed in triplicate)

Interaction between ECs and rBMSCs, rADSCs, and rSCs in the coculture system

Matrigel tube formation assay was performed to evaluate the effects of EC-stem cell coculture on tube formation. Therefore, HUVECs pre-labeled with Cell-Tracker™ CM-Dil were mixed with rBMSCs$^{GFP+/+}$, rSCs$^{GFP+/+}$, and rADSCs$^{GFP+/+}$ at a ratio of 4:1. Within the first 16 h of seeding on Matrigel, the development of neo-capillary networks with well-formed lumens was observed. The lumen of tubular-like structures was paved by ECs, while rBMSCs$^{GFP+/+}$, rSCs$^{GFP+/+}$, and rADSCs$^{GFP+/+}$ immediately migrated toward the lumens and then elongated, co-aligned, and ultimately intercalated among the ECs, although aggregated cells were occasionally present (Fig. 2). Moreover, compared to the EC monoculture, the formation of vascular-like networks was remarkably enhanced in the coculture conditions. The rBMSC- and rADSC-HUVEC cocultures exhibited a significantly improved tubulogenesis scoring ($P=0.023$ and $P=0.034$, respectively) as well as increased tube length ($P=0.034$ and $P=0.041$, respectively) compared with the HUVEC monoculture, whereas the rSC-HUVEC coculture resulted in a non-significant difference in Matrigel tube formation 16 h after seeding (Fig. 3a–f). Our results also showed that none of the adult stem cells had a stimulatory effect on endothelial proliferation in the EC-stem cell coculture systems (Fig. 4). Specifically, in the rBMSC-HUVEC coculture, some dual-fluorescent cells were discernible, indicating that extensive cell-cell cross-talks occurred between rBMSC and EC (Fig. 2c"). Vesicle trafficking between adjacent stem cell-EC, in addition to cell-cell

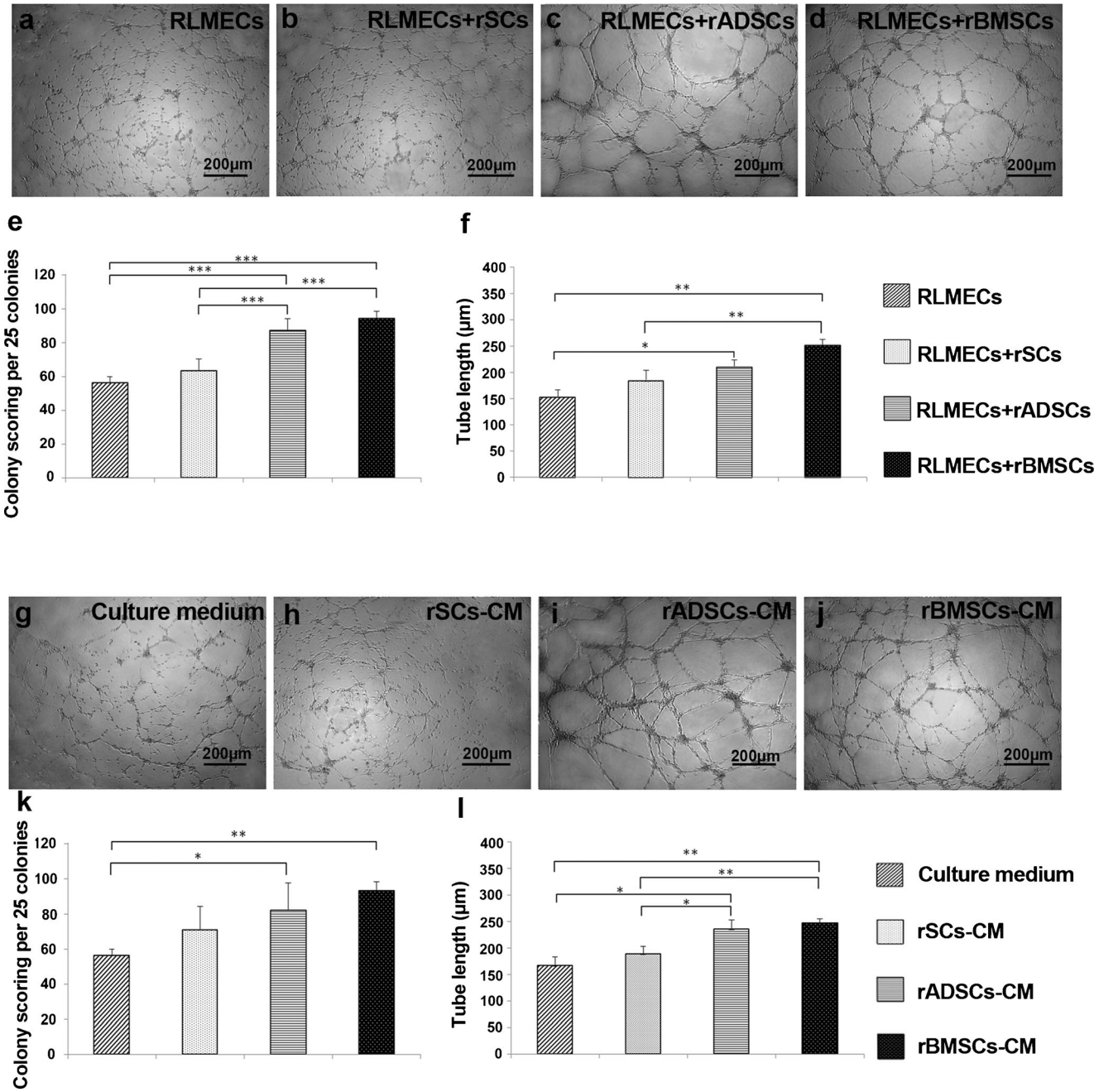

Fig. 5 Effects of tissue-specific stem cells and their conditioned media (CM) on the tubulogenic properties of RLMECs. Tube formation properties (**e**, **f**) of RLMECs were significantly improved when RLMECs were cocultured with rBMSCs (**d**) or rADSCs (**c**) compared with the control monoculture (**a**) or RLMECs-rSCs coculture (**b**). Promotion of tubulogenesis score (**k**) as well as tube length (**l**) for RLMECs incubated with the CM from marrow- (**j**) and adipose-derived stem cells (**i**). Data are expressed as mean±SD (three independent experiments were performed in triplicate). *$P<0.05$, **$P<0.01$, ***$P<0.001$ (one-way ANOVA with bonferroni post hoc test)

connection and juxtacrine interactions, may contribute to the modulation of endothelial angiogenic response (Aguirre et al. 2010).

Likewise, the allogeneic coculture of RLMECs with the rat tissue-specific stem cells showed that the rBMSCs and rADSCs had superior effects on the Matrigel tube formation properties of the RLMECs (Fig. 5a-f).

Pro-angiogenic properties of stem cell-CM

In order to explore the paracrine interactions of the stem cells used in this study and ECs, endothelial tube formation on Matrigel was assessed after 16 h incubation of HUVECs or RLMECs with the rSCs-, rADSCs-, and rBMSCs-derived CM. Statistical analysis revealed stimulatory effects of all

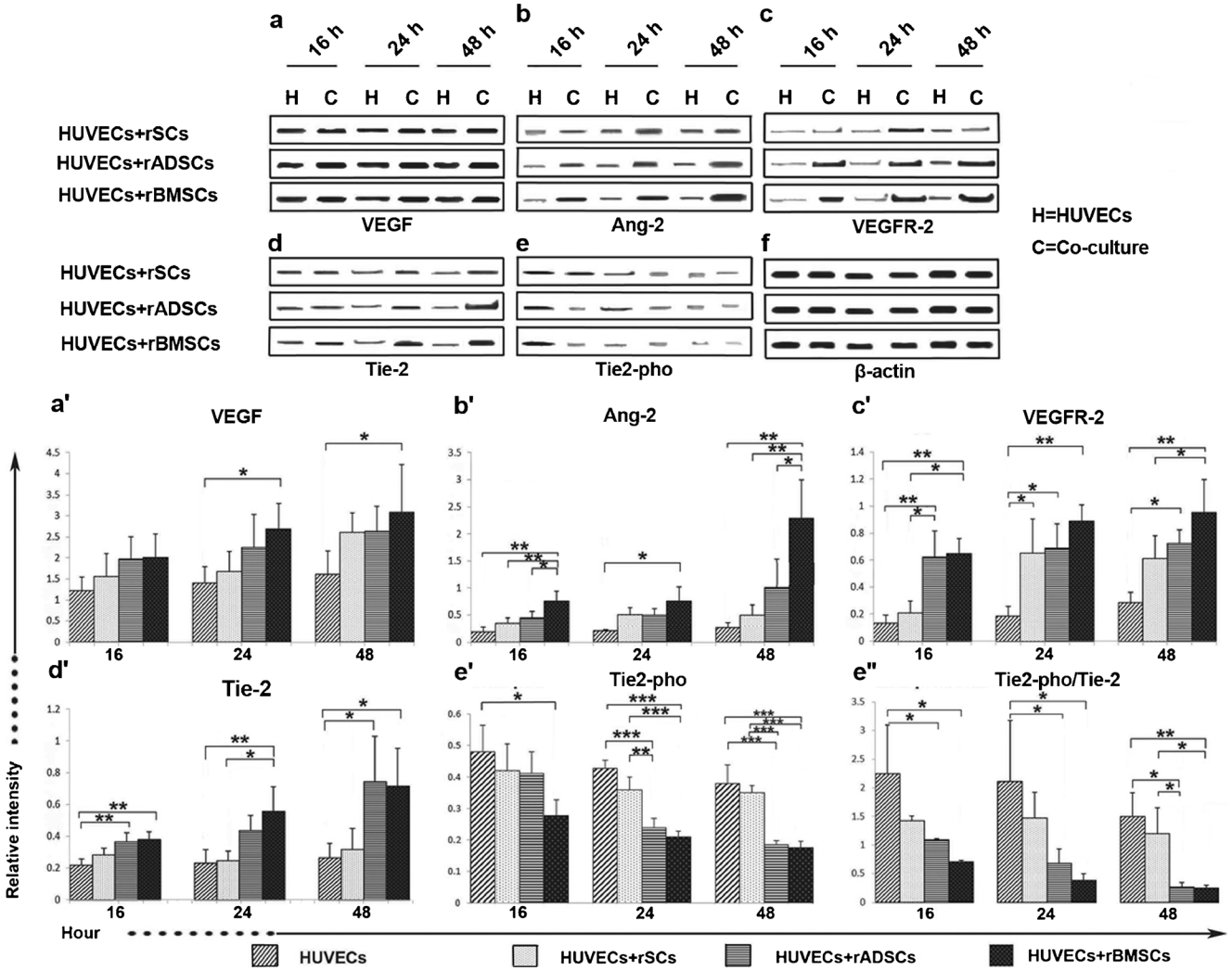

Fig. 6 Changes in vascular endothelial growth factor (*VEGF*), angiopoietin 2 (*Ang-2*), vascular endothelial growth factor receptor 2 (*VEGFR-2*), Tie-2, Tie2-pho, and the Tie2-pho/Tie-2 ratio after HUVECs juxtaposition with tissue stem cells. Western blot analysis shows the dynamic up-regulation of VEGF (**a**, **a'**), Ang-2 (**b**, **b'**), VREGR-2 (**c**, **c'**), and Tie-2 (**d**, **d'**) and the dynamic down-regulation of Tie2-pho (**e**, **e'**) and the Tie2-pho/Tie-2 ratio (**e''**) in ECs when HUVECs were cocultured with tissue stem cells. Western blotting was performed on CD31 positive cells sorted from HUVECs or from HUVECs cocultures with stem cells. Molecular weights of the immunoreactive bands are as follows: VEGF≃42kD, Ang-2≃63, VEGFR-2≃150, Tie-2≃126, and Tie-pho≃126. The *Y*-axis stands for arbitrary units. After band densitometry, the area under the curve of each band was divided by the area under the curve of the corresponding actin band (**f**), and the calculated values were compared between the groups. Data are from three independent experiments (quintuplicate samples for each group in each time point). Data are expressed as mean±SD. **P*<0.05, ***P*<0.01, and ****P*<0.001 (one-way ANOVA with Bonferroni post hoc test)

CM on endothelial tubulogenesis scoring as well as on tube length, with the rBMSCs-CM possessing the strongest pro-angiogenic activities (Figs. 3g–l, 5g–l). Intriguingly, CM from the tissue-specific stem cells had a similar effect on the HUVECs and RLMECs, although the length of the tubes formed by the RLMECs was greater than that by the HUVECs.

Kinetics of angiogenesis signaling in the EC-stem cell coculture system

After coculturing each stem cell with HUVECs, sorting for GFP-negative cells was performed. The sorted CD31-positive ECs were then subjected to western blotting to analyze the endothelial kinetics of key angiogenesis signaling molecules, including VEGF, Ang-1, Ang-2, VEGFR-1, VEGFR-2, Tie-2, and Tie2-pho, in the EC-stem cell coculture systems. For this purpose, ECs in the 16, 24, and 48 h after EC-stem cell co-cultures were sorted and submitted to western blot analysis. Our findings showed that tissue-derived stem cells used in the experiments altered the expression of the angiogenic factors in ECs (Fig. 6a–e).

Western blotting showed no Ang-1 and VEGFR-1 immunoreactive bands in CD31-positive ECs harvested from the cocultures as well as from the monoculture controls. In all groups, maximum VEGF levels were detected after 48 h.

Endothelial VEGF expression was more prominent in the EC-rBMSCs coculture than in the other coculture systems, and the endothelial VEGF level was significantly augmented in the EC-rBMSCs coculture after 24 and 48 h ($P<0.01$) compared to the EC monoculture (Fig. 6a'). At all three time points, the mean VEGF expression was higher in the EC-rSCs and -rADSCs cocultures than that in the EC monoculture, but it did not reach the significance level (Fig. 6a').

Like VEGF, the endothelial Ang-2 expression level was greater in the EC-stem cell cocultures at 16, 24, and 48 h and significant changes were detected in the EC-rBMSCs coculture at 16 and 48 h ($P<0.01$) (Fig. 6b'). In addition, the differences in Ang-2 were statistically significant between rBMSCs and rSCs or rADSCs-related cocultures after 16 and 48 h. Our results showed a dynamic rise in the VEGF and Ang-2 expression levels in ECs over time under the influence of stem cells, in particular marrow MSCs. For VEGFR-2, an upward trend was also observed in the coculture systems with the most significant level in the presence of marrow-derived MSCs (Fig. 6c').

Like pro-angiogenic factors, the endothelial Tie-2 receptor exhibited an upward trend over time (Fig. 6d'). Meanwhile, the rBMSCs and rADSCs further augmented the level of Tie-2 in ECs (Fig. 6d'). However, the rSCs failed to alter Tie-2 expression when compared with the EC monoculture.

Western blot analysis revealed that the endothelial Tie2-pho level was decreased in the coculture systems compared to the control monocultures after 16, 24, and 48 h (Fig. 6e'). The reduction in the phosphorylation of Tie-2 in the ECs was effectively significant by rADSCs after 16, 24, and 48 h ($P_{16}<0.05$, $P_{24}<0.001$, and $P_{48}<0.001$) as well as by rBMSCs ($P_{16}<0.01$, $P_{24}<0.001$, and $P_{48}<0.001$) compared to the control monocultures. Indeed, the Tie2-pho/Tie-2 ratio in the ECs was decreased when the ECs were cocultured with tissue-derived stem cells (Fig. 6e''). Meanwhile, significant changes were noted for the rBMSCs ($P_{16}<0.05$, $P_{24}<0.05$, and $P_{48}<0.01$) and rADSCs ($P_{16}<0.05$, $P_{24}<0.05$, and $P_{48}<0.01$).

Discussion

To date, accumulating evidence demonstrates that angiogenesis switching on/off is governed by orchestrated interactions between endogenous pro- and anti-angiogenic factors (Xie et al. 2011). Deciphering the kinetics of pro- and anti-angiogenic factors in physiological and pathological neo-angiogenesis enables us to modulate this intricate phenomenon in different tissue pathologies. In this regard, tissue-derived stem cells are heralded as a source of great promise for augmenting or harnessing neo-angiogenesis. In the present study, the effects of rBMSCs, rADSCs, and rSCs on the kinetics of angiogenesis signals in ECs were investigated via xenogeneic coculture systems with rat and human cells. For this purpose, we focused on key angiogenic signaling molecules, including VEGF and Ang-2, along with their counter-receptors, VEGFR-2 and Tie-2.

Our findings revealed improvement in endothelial tube-like array by rBMSCs and rADSCs, achieved in both juxtacrine and paracrine manners. The pro-angiogenic properties of these cells have also been reported by some previous authors (Duffy et al. 2009; Kachgal and Putnam 2011; Matsuda et al. 2013; Rahbarghazi et al. 2013; Sorrell et al. 2009). For rSCs, however, the paracrine pro-angiogenic activity was more potent than direct rSC-EC interaction. Using EC-stem cell coculture systems, we also demonstrated self-assembled and elongated tube-like structures formed by intimate contact between stem cells and ECs soon after seeding on Matrigel. Moreover, the presence of dual-fluorescent cells in the HUVEC-rBMSC cocultures further affirmed cell-to-cell dye communication and intercellular trafficking between stem cell-ECs, which may partially be mediated by microvesicles and nano-sized exosomes (Zhang et al. 2012). Exosomes transfer a number of molecules, including proteins, RNAs, and microRNAs, between adjacent cells (Otsu et al. 2009; Zhang et al. 2012). Some authors have even indicated that juxtacrine interactions via gap junctions could transfer cell organelles; for example, mitochondria, from MSCs to adjacent cells (Otsu et al. 2009). Gap-junctions were also involved in juxtacrine interactions between rBMSCs and HUVECs (Otsu et al. 2009).

Our results showed that marrow and adipose tissue MSCs were more able to induce a pro-angiogenic response in ECs than muscle-derived stem cells. Interestingly, similar results were obtained when tissue-specific rat stem cells were cocultured with both xenogeneic and allogeneic ECs. These findings further confirmed marrow- and adipose-derived MSCs as potential candidates for promoting angiogenesis in regenerative medicine. Previous investigations have also reported that MSCs displayed vascular cell phenotypes upon interaction with endothelial matrix in the EC-MSC coculture (Lozito et al. 2009). In this context, the endothelial differentiation of MSCs could be triggered through the contact of ECM proteins with MSC surface and the induction of intracellular mechano-transduction pathways (Barker 2011; Nassiri and Rahbarghazi 2014).

According to the results of the present study, rBMSCs and rADSCs simultaneously enhanced the endothelial expression levels of VEGF, Ang-2, VEGFR-2, and Tie-2, whereas these cells reduced Tie2-pho in HUVECs. The concentration of VEGF, Ang-2, and VEGFR-2 signal proteins started to increase in ECs after 16 h of the EC-stem cell cocultures, and then, after a continuous rise, reached a maximum level by 48 h. Taken together, these findings suggest that VEGF, Ang-2, and VEGFR-2 might exert their pro-angiogenic effects synergically (Hata et al. 2004). It seems that the sustained increase of VEGF and Ang-2, coupled with the reciprocal

decrease of the Tie2-pho/Tie-2 ratio, had a pivotal role for establishing a pro-angiogenic milieu (Lobov et al. 2002). Besides the upward expression of Tie-2 by HUVECs on Matrigel over time, the juxtaposition of the stem cells with ECs further enhanced the expression of Tie-2, while rBMSCs and rADSCs strongly decreased the Tie2-pho/Tie-2 ratio. The reduction in the Tie2-pho/Tie-2 ratio can partially be related to the up-regulation of Ang-2, a negative regulator of Tie-2 phosphorylation (Bogdanovic et al. 2006; Felcht et al. 2012). As some recent findings have described both agonistic and antagonistic effects of Ang-2 on Tie-2 receptor in a context-dependent manner (Chen et al. 2004), it seems that the co-activation of other signaling pathways, for example VEGF, might have a modulatory effect on Tie-2 signaling.

Consistent with the results of the current study, it was demonstrated that the transplantation of marrow MSCs in myocardial infarction dynamically induced a pro-angiogenic milieu in the injured myocardium through activation of the VEGF signaling and increasing the Ang2/Ang1 ratio, leading to a decreased Tie2-pho/Tie-2 ratio (Rahbarghazi et al. 2014). Meanwhile, MSCs from different tissues may have different biological effects on tumor angiogenesis. The coculture of human umbilical cord blood-derived MSCs with glioma cells resulted in the induction of apoptosis in tumor cells via tumor necrosis factor-related apoptosis-inducing ligand (TRAIL) with subsequent inhibition of tumor growth, whereas ADSCs promoted glioma growth, which was associated with the overexpression of some pro-angiogenic factors, including VEGF, Ang1, PDGF-α, PDGF-β, IGF, and SDF-1 (Akimoto et al. 2013). In addition, the secretion of pro-angiogenic factors, including VEGF and Ang1, by bone marrow MSCs was shown to play a pivotal role in the recruitment and proliferation of ECs and keratinocytes in the mouse excisional wound splinting model, leading to accelerated neo-angiogenesis and wound healing (Chen et al. 2008; Wu et al. 2007).

The results of the present study showed that tissue-derived stem cells are potent regulators of the endothelial cell function. The activation of VEGF and Ang-2 signalings in ECs by marrow- and adipose-derived MSCs indicates the importance of the stem cell milieu in the induction of neo-angiogenesis. As the induction or modulation of angiogenesis is an outstanding therapeutic target in many diseases, adult stem cells should be considered as an important strategy to regulate the endothelial function in angiogenesis. For this purpose, interactions between stem cells and ECs need to be clarified in different physiopathological conditions.

Acknowledgments We extend our appreciation to Mr. Ehsan Janzamin and Mrs. Maryam Zakipour for their technical assistance. This study was supported by a research grant from the University of Tehran.

References

Agorogiannis G, Alexaki V, Castana O, Kymionis G (2012) Topical application of autologous adipose-derived mesenchymal stem cells (MSCs) for persistent sterile corneal epithelial defect. Graefes Arch Clin Exp Ophthalmol 250:455–457

Aguirre A, Planell JA, Engel E (2010) Dynamics of bone marrow-derived endothelial progenitor cell/mesenchymal stem cell interaction in co-culture and its implications in angiogenesis. Biochem Biophys Res Commun 400:284–291

Akimoto K, Kimura K, Nagano M, Takano S, To'a Salazar G, Yamashita T, Ohneda O (2013) Umbilical cord blood-derived mesenchymal stem cells inhibit, but adipose tissue-derived mesenchymal stem cells promote, glioblastoma multiforme proliferation. Stem Cells Dev 22:1370–1386

Baraniak P, McDevitt T (2010) Stem cell paracrine actions and tissue regeneration. Regen Med 5:121–143

Barbash IM, Chouraqui P, Baron J, Feinberg MS, Etzion S, Tessone A, Miller L, Guetta E, Zipori D, Kedes LH, Kloner RA, Leor J (2003) Systemic delivery of bone marrow–derived mesenchymal stem cells to the infarcted myocardium: feasibility, cell migration, and body distribution. Circulation 108:863–868

Barker TH (2011) The role of ECM proteins and protein fragments in guiding cell behavior in regenerative medicine. Biomaterials 32: 4211–4214

Baudin B, Bruneel A, Bosselut N, Vaubourdolle M (2007) A protocol for isolation and culture of human umbilical vein endothelial cells. Nat Protoc 2:481–485

Bogdanovic E, Nguyen VP, Dumont DJ (2006) Activation of Tie2 by angiopoietin-1 and angiopoietin-2 results in their release and receptor internalization. J Cell Sci 119:3551–3560

Boomsma RA, Geenen DL (2012) Mesenchymal stem cells secrete multiple cytokines that promote angiogenesis and have contrasting effects on chemotaxis and apoptosis. PLoS ONE 7, e35685

Chen JX, Chen Y, DeBusk L, Lin W, Lin PC (2004) Dual functional roles of Tie-2/angiopoietin in TNF-α-mediated angiogenesis. Am J Physiol Heart Circ Physiol 287:H187–H195

Chen L, Tredget EE, Wu PY, Wu Y (2008) Paracrine factors of mesenchymal stem cells recruit macrophages and endothelial lineage cells and enhance wound healing. PLoS ONE 3, e1886

Danoviz M, Yablonka-Reuveni Z (2012) Skeletal muscle satellite cells: background and methods for isolation and analysis in a primary culture system. Methods Mol Biol 798:21–52

Davis GE, Senger DR (2005) Endothelial extracellular matrix: biosynthesis, remodeling, and functions during vascular morphogenesis and neovessel stabilization. Circ Res 97:1093–1107

Deng J, Han Y, Yan C, Tian X, Tao J, Kang J, Li S (2010) Overexpressing cellular repressor of E1A-stimulated genes protects mesenchymal stem cells against hypoxia- and serum deprivation-induced apoptosis by activation of PI3K/Akt. Apoptosis 15:463–473

Duffy GP, Ahsan T, O'Brien T, Barry F, Nerem RM (2009) Bone marrow–derived mesenchymal stem cells promote angiogenic processes in a time-and dose-dependent manner in vitro. Tissue Eng A 15: 2459–2470

Felcht M, Luck R, Schering A, Seidel P, Srivastava K, Hu J, Bartol A, Kienast Y, Vettel C, Loos EK, Kutschera S, Bartels S, Appak S, Besemfelder E, Terhardt D, Chavakis E, Wieland T, Klein C, Thomas M, Uemura A, Goerdt S, Augustin HG (2012) Angiopoietin-2 differentially regulates angiogenesis through TIE2 and integrin signaling. J Clin Invest 122:1991–2005

Hakamata Y, Tahara K, Uchida H, Sakuma Y, Nakamura M, Kume A, Murakami T, Takahashi M, Takahashi R, Hirabayashi M, Ueda M, Miyoshi I, Kasai N, Kobayashi E (2001) Green fluorescent protein-transgenic rat: a tool for organ transplantation research. Biochem Biophys Res Commun 286:779–785

Hata K, Nakayama K, Fujiwaki R, Katabuchi H, Okamura H, Miyazaki K (2004) Expression of the angopoietin-1, angopoietin-2, Tie2, and vascular endothelial growth factor gene in epithelial ovarian cancer. Gynecol Oncol 93:215–222

Ho IA, Toh HC, Ng WH, Teo YL, Guo CM, Hui KM, Lam PY (2013) Human bone marrow-derived mesenchymal stem cells suppress human glioma growth through inhibition of angiogenesis. Stem Cells 31:146–155

Hsiao ST, Asgari A, Lokmic Z, Sinclair R, Dusting GJ, Lim SY, Dilley RJ (2012) Comparative analysis of paracrine factor expression in human adult mesenchymal stem cells derived from bone marrow, adipose, and dermal tissue. Stem Cells Dev 21:2189–2203

Kachgal S, Putnam A (2011) Mesenchymal stem cells from adipose and bone marrow promote angiogenesis via distinct cytokine and protease expression mechanisms. Angiogenesis 14:47–59

Kinnaird T, Stabile E, Burnett MS, Lee CW, Barr S, Fuchs S, Epstein SE (2004) Marrow-derived stromal cells express genes encoding a broad spectrum of arteriogenic cytokines and promote in vitro and in vivo arteriogenesis through paracrine mechanisms. Circ Res 94: 678–685

Lobov IB, Brooks PC, Lang RA (2002) Angiopoietin-2 displays VEGF-dependent modulation of capillary structure and endothelial cell survival in vivo. Proc Natl Acad Sci U S A 99:11205–11210

Lozito TP, Kuo CK, Taboas JM, Tuan RS (2009) Human mesenchymal stem cells express vascular cell phenotypes upon interaction with endothelial cell matrix. J Cell Biochem 107:714–722

Magee JC, Stone AE, Oldham KT, Guice KS (1994) Isolation, culture, and characterization of rat lung microvascular endothelial cells. Am J Physiol Lung Cell Mol Physiol 267:L433–L441

Marin V, Kaplanski G, Grès S, Farnarier C, Bongrand P (2001) Endothelial cell culture: protocol to obtain and cultivate human umbilical endothelial cells. J Immunol Methods 254:183–190

Matsuda K, Falkenberg KJ, Woods AA, Choi YS, Morrison WA, Dilley RJ (2013) Adipose-derived stem cells promote angiogenesis and tissue formation for in vivo tissue engineering. Tissue Eng A 19:1327–1335

Meligy F, Shigemura K, Behnsawy H, Fujisawa M, Kawabata M, Shirakawa T (2012) The efficiency of in vitro isolation and myogenic differentiation of MSCs derived from adipose connective tissue, bone marrow, and skeletal muscle tissue. In Vitro Cell Dev Biol Anim 48:203–215

Mima Y, Fukumoto S, Koyama H, Okada M, Tanaka S, Shoji T, Emoto M, Furuzono T, Nishizawa Y, Inaba M (2012) Enhancement of cell-based therapeutic angiogenesis using a novel type of injectable scaffolds of hydroxyapatite-polymer nanocomposite microspheres. PLoS ONE 7, e35199

Nassiri SM, Rahbarghazi R (2014) Interactions of mesenchymal stem cells with endothelial cells. Stem Cells Dev 23:319–332

Otsu K, Das S, Houser SD, Quadri SK, Bhattacharya S, Bhattacharya J (2009) Concentration-dependent inhibition of angiogenesis by mesenchymal stem cells. Blood 113:4197–4205

Rahbarghazi R, Nassiri SM, Khazraiinia P, Kajbafzadeh AM, Ahmadi SH, Mohammadi E, Molazem M, Zamani-Ahmadmahmudi M (2013) Juxtacrine and paracrine interactions of rat marrow-derived mesenchymal stem cells, muscle-derived satellite cells, and neonatal cardiomyocytes with endothelial cells in angiogenesis dynamics. Stem Cells Dev 22:855–865

Rahbarghazi R, Nassiri SM, Ahmadi SH, Mohammadi E, Rabbani S, Araghi A, Hosseinkhani H (2014) Dynamic induction of pro-angiogenic milieu after transplantation of marrow-derived mesenchymal stem cells in experimental myocardial infarction. Int J Cardiol 173:453–466

Rhoads RP, Johnson RM, Rathbone CR, Liu X, Temm-Grove C, Sheehan SM, Hoying JB, Allen RE (2009) Satellite cell-mediated angiogenesis in vitro coincides with a functional hypoxia-inducible factor pathway. Am J Physiol Cell Physiol 296:C1321–C1328

Salvucci O, Yao L, Villalba S, Sajewicz A, Pittaluga S, Tosato G (2002) Regulation of endothelial cell branching morphogenesis by endogenous chemokine stromal-derived factor-1. Blood 99:2703–2711

Sambasivan R, Yao R, Kissenpfennig A, Van Wittenberghe L, Paldi A, Gayraud-Morel B, Guenou H, Malissen B, Tajbakhsh S, Galy A (2011) Pax7-expressing satellite cells are indispensable for adult skeletal muscle regeneration. Development 138:3647–3656

Sorrell JM, Baber MA, Caplan AI (2009) Influence of adult mesenchymal stem cells on in vitro vascular formation. Tissue Eng A 15:1751–1761

Taha MF, Hedayati V (2010) Isolation, identification and multipotential differentiation of mouse adipose tissue-derived stem cells. Tissue Cell 42:211–216

Tang J, Wang J, Yang J, Kong X, Zheng F, Guo L, Zhang L, Huang Y (2009) Mesenchymal stem cells over-expressing SDF-1 promote angiogenesis and improve heart function in experimental myocardial infarction in rats. Eur J Cardiothorac Surg 36:644–650

Villars F, Guillotin B, Amédée T, Dutoya S, Bordenave L, Bareille R, Amédée J (2002) Effect of HUVEC on human osteoprogenitor cell differentiation needs heterotypic gap junction communication. Am J Physiol Cell Physiol 282:C775–C785

Wu Y, Chen L, Scott PG, Tredget EE (2007) Mesenchymal stem cells enhance wound healing through differentiation and angiogenesis. Stem Cells 25:2648–2659

Xie L, Duncan MB, Pahler J, Sugimoto H, Martino M, Lively J, Mundel T, Soubasakos M, Rubin K, Takeda T (2011) Counterbalancing angiogenic regulatory factors control the rate of cancer progression and survival in a stage-specific manner. Proc Natl Acad Sci U S A 108:9939–9944

Zhang HC, Liu XB, Huang S, Bi XY, Wang HX, Xie LX, Wang YQ, Cao XF, Lv J, Xiao FJ, Yang Y, Guo ZK (2012) Microvesicles derived from human umbilical cord mesenchymal stem cells stimulated by hypoxia promote angiogenesis both in vitro and in vivo. Stem Cells Dev 21:3289–3297